Physics of the Earth and Planetary Interiors 289 (2019) 34–44

Contents lists available at ScienceDirect

Physics of the Earth and Planetary Interiors

journal homepage: www.elsevier.com/locate/pepi

A reappraisal of the 1978 *Ferruzzano* earthquake (southern Italy) from new estimates of hypocenter location and moment tensor inversion

Barbara Orecchio[a,*], Silvia Scolaro[a], Josep Batlló[b], Graziano Ferrari[c], Debora Presti[a], Daniel Stich[d]

[a] Department of Mathematics, Computer Sciences, Physics, and Earth Sciences, University of Messina, Viale F. Stagno D'Alcontres 31, Messina, Italy
[b] Institut Cartogràfic i Geològic de Catalunya, Barcelona, c. Balmes 209-211, E-08006 Barcelona, Spain
[c] Istituto Nazionale di Geofisica e Vulcanologia, Sezione di Bologna, Via Donato Creti 12, Bologna, Italy
[d] Instituto Andaluz de Geofísica, Universidad de Granada, Campus Universitario de Cartuja s/n, E-18071 Granada, Spain

ARTICLE INFO

Keywords:
Moment tensor inversion
Waveform analysis
Analog seismograms
Non-linear hypocenter location
Calabrian Arc region

ABSTRACT

The March 11th, 1978 *Ferruzzano* earthquake is the most recent moderate-to-major earthquake occurred in the southern Calabrian region (southern Italy), one among the highest seismic risk areas of the whole Mediterranean. Previous information available from the literature on the 1978 earthquake is quite contrasting and not well framed in the regional seismotectonic scenario. In the present study we selected and digitized analog seismograms coming from stations of the Euro-Mediterranean region to invert for the deviatoric seismic moment tensor through a time-domain algorithm properly implemented to analyze data recorded before the advent of the digital era. Moreover, we estimated a new hypocentral location by using original bulletin data and a non-linear probabilistic earthquake location technique working with 3D velocity models. The quality and stability of the obtained results, both for hypocenter location and moment tensor inversion, were accurately checked by several inversion tests. Our results indicate that the 1978 earthquake (i) occurred westward and at a shallower depth respect to previous hypocenter locations, (ii) is characterized by a ca. N-S trending normal faulting mechanism and (iii) has a moment magnitude of 4.7, thus suggesting an overestimate of previous evaluations. This study furnishes new information on the 1978 *Ferruzzano* earthquake allowing to better frame it in the regional seismotectonic scenario and also proves that the time-domain waveform inversion algorithm applied to digitized old seismograms is capable to successfully invert also $M_w < 5$ earthquakes. The obtained results pave the way for future analyses of the early instrumental seismicity potentially capable to furnish new constraints to local and regional seismotectonic modeling.

1. Introduction

The Calabrian Arc (Southern Italy) is a sector of the Mediterranean region characterized by a complex geodynamic scenario influenced by the transition between a compressive domain due to the NW-trending Nubia-Eurasia convergence, and an extensional domain related to the residual southeastward rollback of the Ionian lithospheric slab (Fig. 1a). It is a high seismic risk area struck by several destructive earthquakes (up to 7–7.5 magnitude) mainly occurred in historical times (Rovida et al., 2016; Tiberti et al., 2017). Despite the large amount of geological and geophysical studies carried out in this area, both the fault geometry of the strongest earthquakes and the relationship between large-scale geodynamics and more localized seismogenic processes is still largely debated (Billi et al., 2010; Galli et al., 2008; Neri et al., 2004; Palano, 2015; Presti et al., 2017; Tiberti et al., 2017).

In this context, the study of moderate-to-major earthquakes (i.e., $M_w \geq 5$), directly related to the regional-scale processes, may be crucial to better characterize regional seismotectonics and seismic hazard. Only a small number of moderate-to-major earthquakes occurred in the Calabrian Arc region in the last ca. forty years while several $M_w \geq 5$ earthquakes were recorded in the early seismic instrumental periods (see e.g. 1900–1980; Fig. 1b). This makes very precious every effort aimed to accurately investigate these past earthquakes. In the last decades, the scientific community has become increasingly aware of the importance of recovering historical data and many authors have proven the effectiveness of the use of these kind of data in combination with

* Corresponding author.
E-mail addresses: orecchio@unime.it (B. Orecchio), silscolaro@unime.it (S. Scolaro), jbatllo@igc.cat (J. Batlló), graziano.ferrari@ingv.it (G. Ferrari), dpresti@unime.it (D. Presti), stich@ugr.es (D. Stich).

https://doi.org/10.1016/j.pepi.2019.02.003
Received 15 June 2018; Received in revised form 18 January 2019; Accepted 1 February 2019
Available online 23 February 2019
0031-9201/

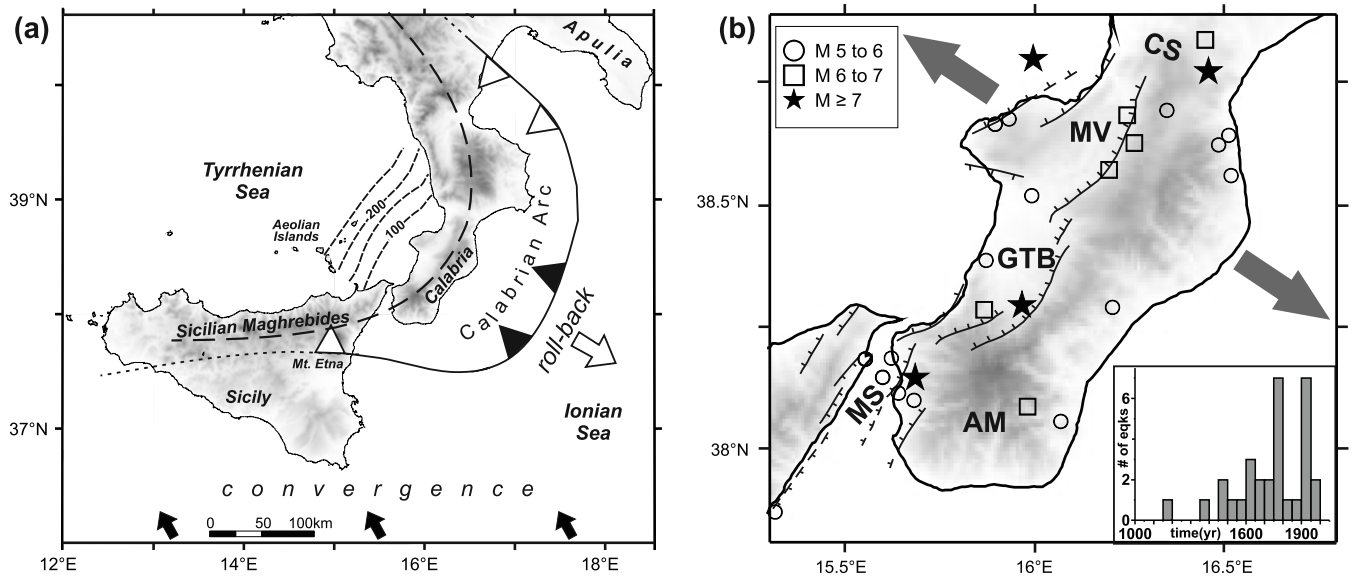

Fig. 1. (a) Map view of the Calabrian Arc region. The solid curve with triangles pointing in the direction of subduction indicates the present-day location of the Ionian subducting system. According to recent literature (see, among others, Neri et al., 2009 and 2012; Orecchio et al., 2014), black triangles indicate the continuous subducting slab while white triangles the plate boundary segments where slab has already undergone detachment. The white arrow shows the sense of the subducting slab rollback. The black arrows indicate the present motion of Nubia relative to Eurasia (Nocquet, 2012, and references therein). The large dashed curve running from Southern Apennines to Sicilian Maghrebides through Calabria indicates the Apennine-Maghrebian chain. Thick dashed lines are depth contour lines of the Wadati-Benioff zone (Faccenna et al., 2011). (b) Enlarged view of the southern Calabria area showing the main fault system (Monaco and Tortorici, 2000) and the earthquakes of magnitude 5.0 and larger that have occurred after 1000 CE, according to the CPTI15 catalog (Rovida et al., 2016). MS = Messina Straits, AM = Aspromonte Massif, GTB = Gioia Tauro Basin, MV = Mesima Valley and CS = Catanzaro Straits. The gray divergent arrows indicate the direction of extension according to seismogenic stress field estimation of Totaro et al. (2016). The inset shows the time distribution of earthquakes reported in map (i.e., M ≥ 5 earthquakes occurred after 1000 CE, from the CPTI15 catalog).

modern techniques of analysis (Batlló et al., 2008, 2010; Okal and Reymond, 2003; Pino et al., 2008; Stich et al., 2003, 2005, 2018; Vannoli et al., 2015, 2016). On this regards, specific projects have been implemented with the aim to collect, recover and store historical seismograms. In particular for the Italian region we may refer to the SISMOS and EuroSeismos Projects (Ferrari and Pino, 2003; Michelini et al., 2005; http://sismos.ingv.it/; http://storing.ingv.it/es_web/) focused on the digitization of seismogram records and seismic bulletins relative to the period 1895–1984, i.e., from the early age of seismometry to the advent of the digital era (Michelini et al., 2005). The availability of these data furnishes the opportunity to investigate not fully resolved earthquakes of the past by using modern technique of analysis.

In this framework we studied the most recent moderate-to-major earthquake included in the SISMOS catalogue for the Calabrian Arc region that is the so called *Ferruzzano* earthquake (Bottari et al., 1981) occurred in southern Calabria on 1978, March 11th (M_w = 5.2, Dziewonski et al., 1987). Contrasting and poorly constrained results have been reported in the literature both concerning hypocenter location and focal mechanism solution of this earthquake (Dziewonski et al., 1987; Gasparini et al., 1985; Rovida et al., 2016). Moreover, framing of the proposed focal mechanisms in the regional seismotectonic scenario appears quite problematic. In this study we estimated for the 1978 earthquake a new hypocenter location by means of Bayloc non-linear probabilistic algorithm (Presti et al., 2004; 2008) and the deviatoric moment tensor by using original seismograms mainly obtained from the SISMOS Project and by applying a time-domain waveform inversion analysis properly calibrated for analog seismic data (Stich et al., 2005).

2. Seismotectonic framework

The Calabrian Arc, southern Italy (Fig. 1a), is the result of the Neogene–Quaternary tectonic convergence between Nubia and Eurasia in the central Mediterranean (Billi et al., 2011; Faccenna et al., 2004; Malinverno and Ryan, 1986; Pepe et al., 2010; Presti et al., 2013; Rosenbaum and Lister, 2004). It is a major tectonic structure uplifting at a rate of 0.5–1.2 mm/yr in the last 1–0.7 Myrs, with internal deformation mainly accommodated by normal faulting (see e.g. Catalano et al., 2003; Monaco and Tortorici, 2000; Neri et al., 2003; 2004). The regional geodynamic model (see, among others, Faccenna et al., 1996; Malinverno and Ryan, 1986; Neri et al., 2005) assumes the co-existence of northwest–southeast convergence of Nubia and Eurasia plates and southeast-ward rollback of the Ionian lithospheric slab subducting to northwest beneath the Tyrrhenian lithosphere (Fig. 1a). The space-time evolution of the rollback process characterized by slab migration and lithospheric tearing have led to a progressive segmentation of the subduction zone. A consequence of this process is that, as shown by recent studies (Neri et al., 2009, 2012; Orecchio et al., 2014; Polonia et al., 2016), the residual descending lithospheric body is located in a small sector beneath southern Calabria (i.e., about between the Catanzaro Straits to the north and the Messina Straits to the south). In this framework the very slow trench retreat is considered however still capable of causing strong normal faulting earthquakes in the southern Calabria region (Orecchio et al., 2014).

The seismic activity of southern Calabria has been characterized by several destructive earthquakes, as clearly shown in Fig. 1(b) reporting $M_w > 5$ events occurred from 1000 to 2016 (Rovida et al., 2016). The latest moderate-to-major earthquake is the *Ferruzzano* one occurred on March 11th, 1978 in the southeasternmost sector of Calabria, while the strongest events (i.e. $M_w \geq 7$) are (i) two events occurred during the seismic sequence of February-March 1783 (Jacques et al., 2001; Tiberti et al., 2017), (ii) the 1905 earthquake (Galli and Molin, 2009; Presti et al., 2017; Riuscetti and Schick, 1975) and (iii) the 1908 Messina Straits earthquake, among the most catastrophic events in Italian history (Billi et al., 2008; Pino et al., 2009). Despite years of seismotectonic studies, the causative faults of these major earthquakes are still unknown or debated (e.g., Billi et al., 2010; Galli et al., 2008; Tiberti

et al., 2017), and this is also due to the lack of coseismic surface faulting (Tiberti et al., 2017; Valensise and Pantosti, 2001). The dominant faulting mechanism, instead is widely shared and indicated as normal faulting (see, e.g., DISS Working Group 2015; Ghisetti, 1984; Neri et al., 2006; Tortorici et al., 1995); in particular, only normal faulting mechanisms have been proposed for M7 earthquakes in the belt. Normal faults located closely west of the chain are considered to be major seismogenic faults, with particular reference to the NE-trending fault systems of the Messina Straits, Gioia Tauro Basin and Mesima Valley (Fig. 1b). The structural setting of the central-eastern portion of southern Calabria is less constrained with respect to the eastern one where major earthquakes have been occurred and main structural systems have been deeply investigated. On overall, geostructural data (Tortorici et al., 1995) provided evidence that the fault systems of southern Calabria are mainly subjected to a ca. SE-NW trending extensional regime.

In spite of the strong historical seismicity, a light to moderate seismic activity has been recorded in the southern Calabria region in recent times with no $M_w > 5$ earthquakes in the last forty years. A huge effort has been devoted to investigate the kinematics of the region by estimating stable and reliable focal mechanism solutions also for such moderate energy seismicity and the results indicate a dominant normal faulting mechanism (D'Amico et al., 2010, 2011; Presti et al., 2013; Totaro et al., 2016). Moreover, the derived seismogenic stress field (Neri et al., 2005; Presti et al., 2013; Totaro et al., 2016) clearly shows a relatively uniform extension with a nearly NW-SE orientation of the minimum compressive stress axis. An extensive regime has been revealed in southern Calabria also by geodetic data, in particular the strain-rate pattern estimated from the GPS-based velocity field clearly shows a positive areal change with maximum extension in the WNW–ESE direction (Chiarabba and Palano, 2017; Palano, 2015; Serpelloni et al., 2010).

3. The *Ferruzzano* earthquake: Previous knowledge

The Ferruzzano earthquake occurred in the Aspromonte area on March 11th 1978, 19:20 GMT (Fig. 2). According to the Parametric Catalogue of Italian Earthquakes (CPTI15; Rovida et al., 2016) the earthquake has been felt in southern Calabria and northeastern Sicily and it has produced a maximum intensity I_{max} = VIII MCS in the villages of Ferruzzano, Bova, Palizzi and Roccaforte del Greco (Fig. 2). Studying the macroseismic field, Bottari et al. (1981 and 1990) evidenced that unfavourable geomorphological and/or hydrogeological conditions in the maximum Intensity area have probably caused an increase in intensity from ca. VII to VIII at the four I_{max} sites. Similar conclusions have also been proposed for the 1907 earthquake (October 23th, $M_w = 6$) occurred approximately in the same epicentral area (Baratta, 1907; Murphy, 1993; Sabatini, 1908).

Macroseismic and instrumental locations indicate the epicentral area of the 1978 earthquake in the central-eastern portion of the Aspromonte region (Fig. 2). The International Seismological Center catalogue (ISC hereafter; http://www.isc.ac.uk/) has previously reported a focal depth of 26 km and magnitude values of $M_s = 5$ and $m_b = 5.5$ (ISC1 in Fig. 2). Just during the revision process of this paper the ISC Bulletin has been rebuilt for the period 1964–1979 and a revised location for the 1978 earthquake is now available (ISC2 in Fig. 2; focal depth of 23.5 km, magnitude values of $M_s = 5.1$ and $m_b = 5.5$). Two quite different focal mechanism solutions are available from the literature. The first one has been obtained by Gasparini et al. (1985) by using ISC1 location and P-onset polarities inversion and it indicates a ca. transpressive mechanism with nodal planes about N-S and E-W oriented (Fig. 2). It is widely known that focal mechanisms elaborated by using P-wave first motions may be strongly biased by data distribution and uncertainty (e.g., Lay and Wallace, 1995; Pondrelli et al., 2006; Scognamiglio et al., 2009; Presti et al., 2013). Moreover, the hypocenter location uncertainty, with particular reference to the focal depth, may influence the estimation of take-off angles and thus the polarity distribution. Concerning Gasparini et al. (1985) solution (G&al hereafter), the authors have not discussed the reliability of the result but the polarity distribution suggests a quite poorly resolved solution characterized by several discrepancies between observed and predicted polarities. The latter is the Centroid Moment Tensor solution (CMT hereafter; Dziewonski et al., 1987; http://www.globalcmt.org) indicating normal faulting on a ca. E-W trending fault plane (Fig. 2) and furnishing moment magnitude $M_w = 5.2$ and depth = 15 km. CMT computes the moment tensors by inverting mantle waves in the band 125–350 s and body waves in the band 40–125 s recorded at teleseismic distances and, only after 2003, even teleseismic surface waves with period 50–150 s (Hjörleifsdóttir and Ekström, 2010). For magnitude less of about 5.5 the amplitudes of mantle waves may be comparable with the noise level for most stations and the CMT solutions of earthquake occurred before 2003 could be constrained only by the body waves. This is the case of the *Ferruzzano* earthquake being the CMT solution obtained by using only body waves from 8 stations.

4. Non-linear hypocenter location

Hypocenter location for the 11 March 1978 earthquake and relative location uncertainty estimate have been performed by the Bayesian non-linear location method Bayloc (Presti et al., 2004; 2008). Starting from seismic phase arrival times at the recording stations, Bayloc computes for an individual earthquake a probability cloud marking the hypocenter location uncertainty. Also, Bayloc estimates the spatial distribution of probability relative to a set of earthquakes by summing the probability densities of the individual events. This method uses a 3D velocity model and it has shown to furnish more reliable locations and hypocentral uncertainties with respect to standard linearized algorithms, especially in suboptimal network conditions (Presti et al., 2004; 2008). Moreover, the continuous character of the output quantities is particularly indicated for seismic-network-testing purposes. Further details on methodological aspects of Bayloc can be found in the above quoted papers.

For hypocenter location of the 1978 earthquake the seismic wave readings furnished by International Seismological Center (ISC; http://www.isc.ac.uk), Istituto Nazionale di Geofisica e Vulcanologia (INGV; http://www.ingv.it) and Messina and Catania Universities (see Neri et al., 2003) have been used. We selected seismic wave arrival times at observatory stations located at distances from the epicentral area not greater than 700 km, approximately (Fig. 3a). At these distances the flat earth model can still be adopted (see e.g. Lay and Wallace, 1995; Snoke and Lahr, 2001). For the earthquake zone and up to epicentral distances of a few hundred kilometers (dashed rectangle in Fig. 3a) the 3D seismic velocity model obtained by Neri et al. (2012) through the integration of crustal (Orecchio et al., 2011) and sub-crustal (Neri et al., 2009) seismotomographic models of the Tyrrhenian region has been used. For surrounding zones including seismic ray travelling to farther stations (Fig. 3a) the ak-135 model (Kennett et al., 1995) was considered.

The obtained solution indicates that the 1978 earthquake occurred in the Aspromonte area, more than 10 km West of the ISC1 epicenter location and in better agreement with the macroseismic and ISC2 epicenter locations, with a maximum probability at depth of 11 km beneath the point of coordinates 38.04° N–15.91° E (Fig. 3b). The related epicentral and focal depth uncertainties estimated by the Bayloc algorithm at the 68% level of confidence are of the order of 4 and 5 km, respectively. The differences between our hypocentral location and previous available instrumental locations should be primarily ascribed to the different features of the location procedures. The ISC results come from a standard linearized location using a 1D velocity model whereas the Bayloc algorithm considers the non-linearity of the location problem and takes into account the complete and often multimodal form of probability density functions (Presti et al., 2008). Moreover,

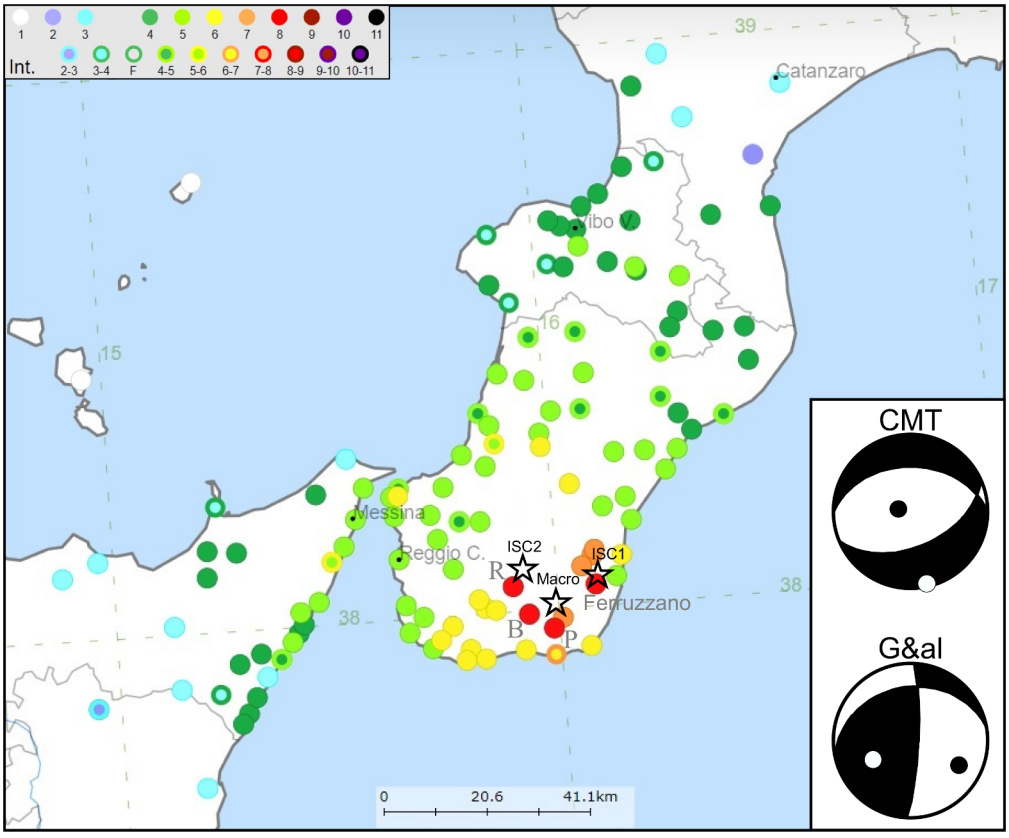

Fig. 2. Macroseismic intensity map of the 1978 earthquake (taken from the Italian Archive of Historical Earthquake Data, https://emidius.mi.ingv.it/ASMI/index_en.htm) also reporting literature information concerning locations and focal mechanisms of the event. R, B and P stand for Roccaforte del Greco, Bova and Palizzi, respectively. Macro, ISC1 and ISC2 indicate the macroseismic location reported by the CPTI15 catalog (Rovida et al., 2016) and the instrumental locations of the International Seismological Center catalog, respectively. The inset shows the focal mechanism solutions furnished by the Centroid Moment Tensor catalogue, CMT in figure (strike/dip/rake 270°/41°/−72°) and by Gasparini et al. (1985), G&al in figure (strike/dip/rake 259°/31°/164°). In the beach-balls we also displayed the P and T axes (black and white circle, respectively).

Bayloc also uses a 3D-velocity structure so allowing a better modelling of the strong heterogeneities characterizing the central Mediterranean region.

Several hypocenter location attempts have been performed for earthquake location by varying the network configuration or by removing outlier data identified through estimated vs. observed arrival time comparison. The hypocentral solutions so obtained appear relatively stable always reporting the epicenter westward with respect to ISC1 location and with hypocenter depths approximately in the range 10–14 km. To further check the dependence of earthquake location from seismic network geometry, we examine the retrieval of several sets of simulated seismic-events recorded by the real seismic network already used (Fig. 3a). For each synthetic event, the arrival times of P and S waves were estimated at the stations used for locating the 11 March 1978 event. A Gaussian noise with standard deviation of 0.2 and 0.5 s was adopted for perturbation of P and S wave readings, respectively. These values of reading errors seem adequate for testing the 1978 hypocenter location taking into account the moderate magnitude of the earthquake and the error reading values discussed in similar conditions (see e.g. for the 1979 Umbrian earthquake, Deschamps et al., 1984). In Fig. 4, we show the results obtained by relocating a group of simulated earthquakes located at different focal depths in the 1978 epicentral area. For each starting location ten synthetic events have been generated with data perturbed by different sets of random noises. The Bayloc relocations of these synthetic events provided a faithful reproduction of the correct hypocenter locations both in map and in depth (Fig. 4) so proving that the network configuration does not produce systematic biases in the hypocenter location.

5. Moment tensor inversion of digitized seismograms

5.1. Data collection

To perform the moment tensor inversion of the 1978 *Ferruzzano* earthquake we collected the original seismograms available from the digital archives of the SISMOS and EuroSeismos Projects (http://sismos.ingv.it/; http://storing.ingv.it/es_web/). In 2001 the INGV started the SISMOS Project focused on digitization and diffusion of seismogram records and bulletins of the Italian seismic observatories relative to the period 1895–1984, that is approximately from the early age of seismometry to the advent of the digital era (Michelini et al., 2005). The Project was extended, in 2002, to seismograms and bulletins from observatories in 28 countries of the Euro-Mediterranean area in the frame of the EuroSeismos project (Ferrari and Pino, 2003). The use of these kind of data needs of particular care being, for example, necessary to properly know the instrumental characteristics of the recording system in order to reconstruct the analytical form of the transfer function (Kanamori, 1988). In the period covered by the SISMOS and EuroSeismos Projects the seismic observatories could be equipped by different type of seismographs and, often, even a same type of instrument could have a different configuration from one observatory to another, thus implying a different transfer function. The instrument information necessary to process the recordings, that were documented manually, sometimes are uncertain or missing and this may preclude the use of the related seismic records. Moreover, the main features of old seismographs could lead to low quality data and/or to data affected by intrinsic uncertainties, such as gaps in the waveform due to time-marks and distortions produced by instrumental limit (Cadek, 1987; Crouse and Matuschka, 1983; Grabrovec and Allegretti, 1994; Herrmann, 1987; Schlupp, 1996). The development of the Worldwide Standardized Seismograph Network (WWSSN) has led, since the sixties, to a progressive improvement of data quality and availability, making available several data in the Euro-Mediterranean area for the 1978 earthquake. Nevertheless, the recording systems were still affected by some of the above discussed problems, therefore the analysis of the 1978 *Ferruzzano* earthquake has required an accurate data selection based on carefully evaluations of each seismogram and of the related instrumental parameters.

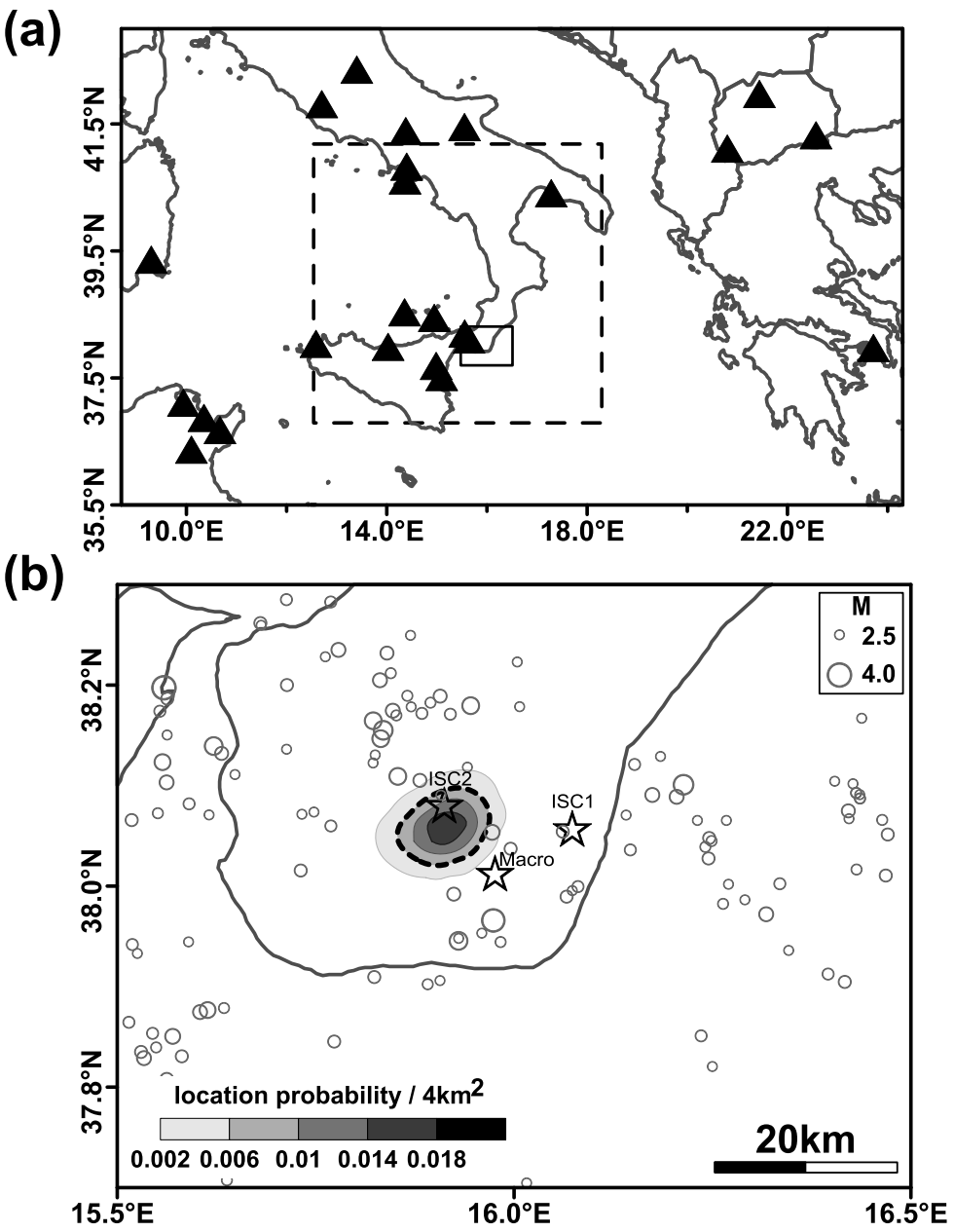

Fig. 3. (a) Map of the seismic stations used in the present study to locate the 1978 earthquake. For hypocenter location, we adopted the local velocity structure of Neri et al. (2012) inside the dashed rectangular area and the ak135 standard velocity model of Kennett et al. (1995) outside. The black contoured rectangle indicates the epicentral area reported in plot b. (b) Results of our Bayesian non-linear hypocenter location reported in terms of location probability per surface unit (4 km^2), with the 68% probability contour evidenced by a black dashed line. Stars indicate the macroseismic (Macro) and the instrumental (ISC1 and ISC2) locations. To better frame the result in the local earthquake distribution we also reported the M ≥ 2.5 earthquakes occurred between 1997 and 2016 (gray circles; data from INGV).

To perform moment tensor inversion by using the time-domain technique of Stich et al. (2005) we selected only the original seismograms recorded by long-period seismographs. The period-band used for waveform modeling (20–50 s) is above the free period of the sensor where the instrumental amplification quickly decreases. This intermediate-period band (20–50 s) is preferred for this kind of inversion because it provides a reasonable compromise between the limited bandwidth of old sensors and an acceptable sensitivity of wave propagation to lateral heterogeneity in the lithosphere (Stich et al., 2003; 2005). We selected the original seismograms characterized by good quality of the recordings and we recovered instrument response parameters from the original station bulletins and from the literature; only in few cases we used the instrument constants reported for the same station in a close time period. Following this approach we selected 16 seismograms from 10 seismic stations (see Table 1 for details on instrumental parameters); in addition to data available from SISMOS and EuroSeismos catalog we also used seismograms of MAL and TOL stations provided by Instituto Geográfico Nacional – Observatorio Geofísico de Toledo. Our dataset mainly consists of waveforms recorded by electromagnetic Sprengnether and Press-Ewing long-period seismographs. For the stations TRI, MAL and TOL the three components of motion are available, for EBR only a single horizontal (N-S) trace and for the remnant stations just the vertical traces. Fig. 5(a) shows the earthquake epicenter location and the network geometry characterized by an azimuthal coverage of about 180° and epicentral distances ranging from ca. 500 to 1970 km. Each seismogram has been digitized manually with the software GIMP (GNU Image Manipulation Program) by redrawing the whole traces. Then it has been interpolated and converted to modern seismological format (i.e., SAC) by TESEO[2] (Turn the Eldest Seismograms into the Electronic Original ones) a GIMP plug-in made up by INGV (Pintore et al., 2005). Finally, all waveforms have been corrected for geometrical distortions and first arrivals have been accurately verified.

5.2. Waveform inversion

The time-domain waveform inversion technique we used to analyze the *Ferruzzano* earthquake, has been properly calibrated to work with

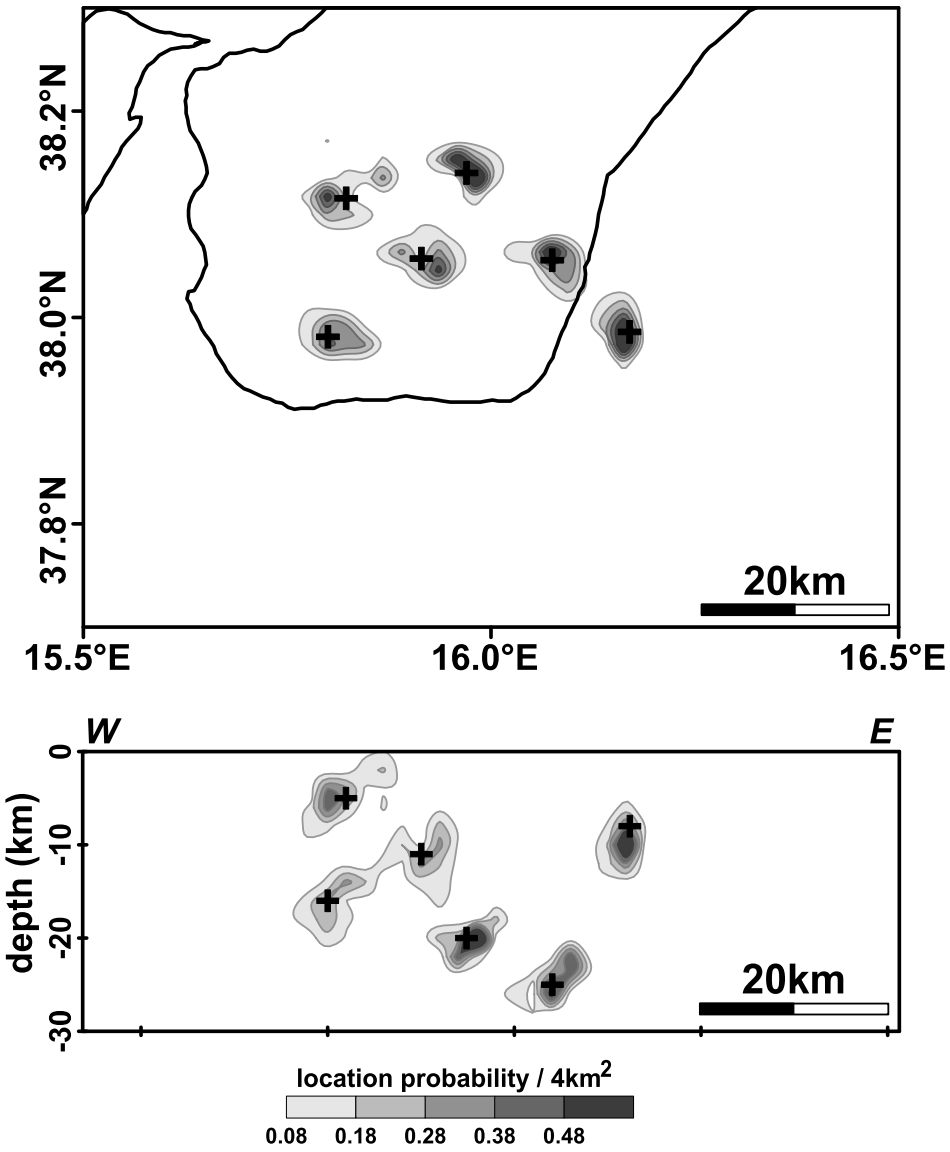

Fig. 4. Map (top) and W-E vertical section (bottom) showing the Bayloc relocations of synthetic events located in the 1978 earthquake area. Crosses indicate the starting position of synthetic earthquakes (note that two starting locations correspond to Bayloc and ISC1 locations of the 1978 earthquake). See Section 4 for further details on the synthetic test.

data collected before the advent of the digital era (Stich et al., 2005). In particular this technique inverts for the deviatoric moment tensor by directly processing the original historical recording without previous rotation of the horizontal seismograms into radial and transverse components. This approach allows preserving all the available waveforms also including those stations where only one horizontal single-component can be recovered, which is the case of station EBR here. Moreover, by using separately each recording it is possible to reduce the errors due to the misalignment of time signals from component to component, wrong polarities and uncertainty of instrumental parameters. The use of historical seismograms processed in the original sensor orientations requires the appropriate treatment of the theoretical Green's functions. The synthetic waveforms are computed for unrotated components (i.e., E, N, Z) and then, processed by convolution to apply the corresponding instrumental response, modelled with poles & zeroes (Batlló and Bormann, 2000; Batlló et al., 2010; Scherbaum, 1996; Stich et al., 2005). To compute the Green's functions we used a specific 1D velocity model for each station (Fig. 5b) estimated as the average model along hypocenter-station path derived from the 1-D global model CRUST2.0 (Bassin et al., 2000). Green's functions calculated from 2 to 30 km depths (every 2 km) were tried successively to find the best combination of focal mechanism and depth. A band-pass filter from 20 s to 50 s has been applied to both the original digitized and synthetic waveforms. During the inversion procedure we assigned different weight factors to the individual waveforms with the aim to take into account data quality, signal amplitudes and waveform fits and also to evaluate the solution stability. The recordings are initially weighted on the basis of original data quality and reliability of the instrumental parameters; then weights are slightly varied by trial and error to improve overall waveform fits and to check the stability of the results (Stich et al., 2005).

We report in Fig. 5c the final focal mechanism solution and the observed-versus-synthetic waveform fits. The best solution for the *Ferruzzano* earthquake indicates normal faulting on a ca. N-trending plane, strike/dip/rake of 352°/20°/−107° and 190°/71°/−84° for the two nodal planes, with an almost horizontal ESE-trending T-axis. The best solution is obtained at a depth of 8 km and the resulting moment magnitude is $M_w = 4.7$ ($M_0 = 0.110 \times 10^{24}$ Nm). The observed-versus-synthetic fits are quite good being the waveforms reproduced adequately at most stations (Fig. 5c). Slightly mismatched phases or small

Table 1
Main parameters of the recording stations used in the present study for moment tensor inversion. Columns report: station code, coordinates, type of instrument, recording component (Comp), free period of the electromagnetic sensor (T_0 S) and of the recording galvanometer (T_0 G), magnification (V), damping constant (ε) and poles and zeroes of the instrument response function we estimated according to Batlló (2004). Star indicates instrumental parameters we inferred from data reported for the same station in a close time period.

STA	Lat (°)	Lon (°)	Instrument	Comp	T_0 S (s)	T_0 G (s)	V	ε	Zeroes	Poles
COP	55.68	12.45	Sprengnether	Z	15	100	1500*	1.0*	0.0 triple	0.4188 ± j0.0000 0.0628 ± j0.0000
EBR	40.82	0.48	Sprengnether	N-S	15	90	1470	0.75	0.0 triple	0.3142 ± j0.2771 0.0524 ± j0.0462
IST	41.05	29.00	Sprengnether	Z	15	100	1500	1.0	0.0 triple	0.4188 ± j0.0000 0.0628 ± j0.0000
LJU	46.04	14.53	Sprengnether	Z	15*	85*	1300*	1.0*	0.0 triple	0.4188 ± j0.0000 0.0739 ± j0.0000
MAL	36.73	−4.41	Sprengnether	E-W, N-S, Z	15	100	1500	1.0	0.0 triple	0.4188 ± j0.0000 0.0628 ± j0.0000
RMP	41.81	12.70	Press-Ewing	Z	15	90	1400	1*	0.0 triple	0.4188 ± j0.0000 0.0698 ± j0.0000
SKO	41.97	21.44	Press-Ewing	Z	15*	100*	1500*	1*	0.0 triple	0.4188 ± j0.0000 0.0628 ± j0.0000
TIM	45.75	21.23	Kirnossystem	Z	25	1.20	500	0.5 (*sensor*) 8.0 (*galvan.*)	0.0 triple	0.1257 ± j0.2177 0.3286 + j0.0000 83.4474 + j0.0000
TOL	39.88	−4.05	Sprengnether	E-W, N-S, Z	15	100	1500	1.0	0.0 triple	0.4188 ± j0.0000 0.0628 ± j0.0000
TRI	45.42	13.46	Press-Ewing	E-W, N-S, Z	15	100	3000	1*	0.0 triple	0.4188 ± j0.0000 0.0628 ± j0.0000

differences in wave amplitudes can be due to crustal structure heterogeneities along the propagation wave paths and to local site effects, respectively. The differences observed at TOL and MAL (components E and Z) seem to indicate a low capability of the sensors to properly recover long wavelength Rayleigh waves, probably as a consequence of the limitations of the instrument sensitivity. The overall level of mismodeling is comparable to other examples of small-magnitude earthquakes recorded at far-regional analog instruments (e.g. Batlló et al., 2010; Stich et al., 2018). Our focal mechanism solution is quite different from the previous available ones (CMT and G&al in Fig. 2). Being not available the original dataset used for the respective analyses (Gasparini et al., 1985; Dziewonski et al., 1987; CMT website), we tried to compare our result with CMT and G&al solutions by evaluating their capability to reproduce waveforms and P-onset polarities of our data (see Figs. S1–S3). We found that the estimated-versus-observed waveform misfits obtained for the previous available solutions (i.e., 1.93 for CMT, 1.39 for G&al) are significantly larger than for our result (0.57 for this study). Moreover, the individual waveform observation and P-onset polarity distributions also show that both of them lead to quite relevant amplitude mismatches and polarity reversals.

The best solution estimated in this study is obtained at a depth of 8 km and the misfit error as function of depth (Fig. 6a) shows that the solution is stable around the minimum. Several tests and trials of inversion have been performed to evaluate reliability and stability of the moment tensor results. By running 100 inversion trials obtained through a bootstrap resampling we have found that 68% of results differ from the best solution of less than 12° in strike, dip and rake. Moreover, we also performed several inversions by slightly changing the weighting factors of the seismograms, the velocity models used for Green's Functions estimate and we tested both different station configurations and epicenter locations. We found that the obtained moment tensor solution, moment magnitude and focal depth are very stable (see few examples reported in Fig. 6b). The use of average velocity model, instead of a specific model for each ray-path, has furnished a slightly different focal mechanism solution and the greatest misfit value (Fig. 6b), so showing the relevance of using an accurate input model in the waveform inversion. The CLVD (Compensated Linear Vector Dipoles) component seems more sensitive to variations but the double-couple constrained inversion (Fig. 6b, bottom) furnished almost the same result of the best solution showing that the earthquake can be modeled as a simple faulting source.

6. Results and discussion

The hypocenter location we obtained by using the probabilistic nonlinear algorithm Bayloc, indicates that the 1978 *Ferruzzano* earthquake occurred approximately in the central-eastern area of the Aspromonte massif. The epicenter is located more than 10 km west of ISC1 instrumental location and closer to the ISC2 and macroseismic one, the hypocenter is about 11 km deep, significantly shallower than previous ISC locations (i.e., 26 and 23.5 km depths). The tests we performed indicate that the obtained solution is well constrained without showing relevant biases due to network geometry. Epicentral and focal depth uncertainties are of the order of 4 and 5 km, respectively.

The moment tensor solution for the 1978 earthquake has been obtained by using a time domain algorithm (Stich et al., 2005) already successfully applied to seismic events occurred before the recording period of modern digital seismometers (see e.g., Batlló et al., 2008; 2010; Stich et al., 2018). The estimated focal mechanism solution indicates normal faulting on a ca. N-S oriented fault plane and it is characterized by an almost horizontal ESE-trending T-axis. We highlight that, in contrast with the focal mechanism solutions previously proposed in the literature (Gasparini et al., 1985; Dziewonski et al., 1987), our result is better framed in the local extensional domain. This is clearly shown by the comparison of T-axis orientations with the extensional directions proposed for southern Calabria by seismologic, geodetic and geologic data (see Fig. 7a). The local geology of the central-eastern portion of southern Calabria is quite debated and different structural settings have been proposed in the literature (see e.g., Ciaranfi et al., 1983; Ghisetti, 1984; Ghisetti and Vezzani, 1981; Van Dijk, 1992). In this framework we cannot uniquely identify a causative fault system but also taking into account these limitations, we highlight the good agreement between our solutions and the structural settings proposed by Ghisetti and Vezzani (1981). In particular the fault plane

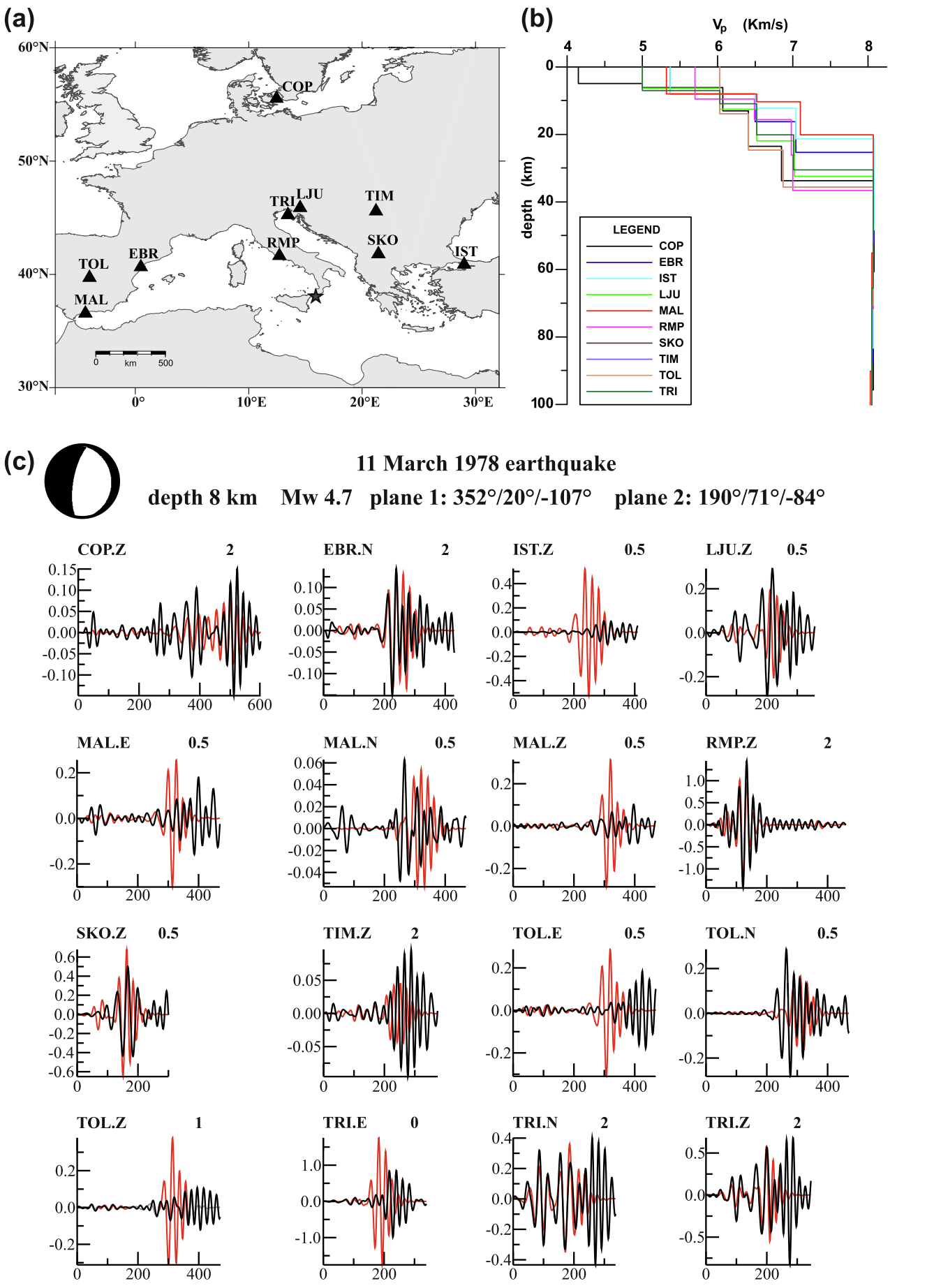

(caption on next page)

Fig. 5. (a) Map showing epicenter location of the 11 March 1978 earthquake as obtained in this study (star) and the seismic stations used for moment tensor inversion (triangles). Data relative to MAL and TOL have been furnished by Instituto Geográfico Nacional - Observatorio Geofísico de Toledo; other data by the SISMOS database of Istituto Nazionale di Geofisica e Vulcanologia. (b) 1D velocity models used to compute the Green's functions for each station and estimated as the average model along hypocenter-station path. (c) Best focal mechanism solution estimated for the 1978 earthquake together with the related waveform fits obtained from the moment tensor inversion. The observed waveforms are indicated by black lines and predicted by red ones; displacement (y-axis) is in millimeters and time (x-axis) in seconds. Above each trace the station code and the weighting factor for inversion are reported. All traces start at the P waves arrival time.

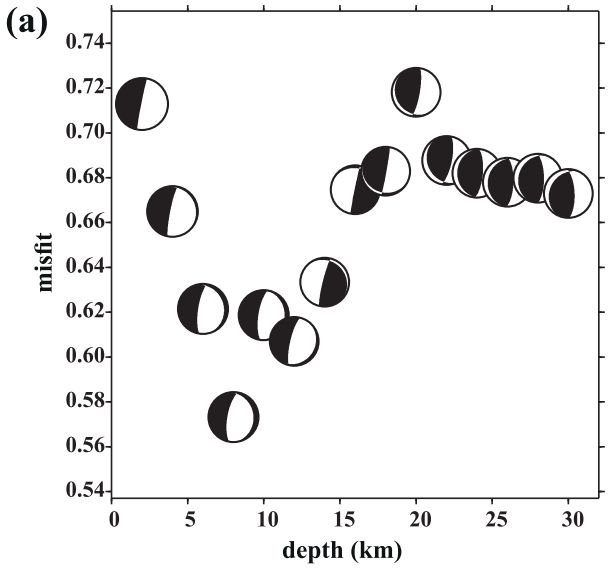

(b)

Best solution CLVD 19.8% - misfit 0.57 - depth 8 km M_w 4.7 - 352°/20°/ -107° 190°/71°/ -84°
Epicenter location ISC1 CLVD 13.5% - misfit 0.61- depth 8 km M_w 4.7 - 356°/ 19°/ 256° 190°/ 71°/ -85°
Stations used **RMP-TRI-LJU-COP-TIM-SKO-IST** CLVD 12.3% - misfit 0.57 - depth 8 km M_w 4.7 - 350°/23°/-106° 188°/68°/-83°
Stations used **TOL-MAL-EBR-RMP-TRI-LJU-COP** CLVD 10.9% - misfit 0.55 - depth 8 km M_w 4.7 - 358°/17°/-98° 187°/73°/-87°
Stations used **EBR-RMP-TRI-LJU-COP-TIM** CLVD 8.6% - misfit 0.50 - depth 8 km M_w 4.7 - 358°/18°/-98° 186°/72°/-87°
Average velocity model CLVD 10.1% - misfit 0.76 - depth 4 km M_w 4.6 - 342°/48°/-106° 185°/44°/-73°
Weighting scheme **COP-EBR-IST-LJU-MAL-RMP-SKO-TIM-TOL-TRI(NZ)= 2** **TRI(E)= 0** CLVD 28.8% - misfit 0.60 - depth 8 km M_w 4.7 - 354°/18°/251° 193°/73°/-84°
Weighting scheme **COP-EBR-IST-RMP-TIM-TOL-TRI(NZ)= 2** **LJU-MAL-SKO= 0.5 TRI(E)= 0** CLVD 41% - misfit 0.62 - depth 8 km M_w 4.7 - 356°/20°/246° 201°/72°/-81°
DC solution misfit 0.56 - depth 4 km M_w 4.6 - 200°/70°/-80° 353°/22°/-116°

Fig. 6. (a) Misfit error as function of depth. The plot shows the stability of the solution around the minimum. (b) Results of tests performed by changing epicenter location, station configurations (also using unfavorable conditions), weighting factors and velocity model used for Green's Function computation. The result obtained for a double-couple constrained inversion is also reported.

orientation depicted by our moment tensor solution matches very well with the N- to NE-trending lineaments reported by Ghisetti and Vezzani (1981) near the Bayloc epicenter location of the 1978 earthquake (see Fig. 7b).

The best focal mechanism solution also indicates a focal depth of 8 km, fully compatible with the Bayloc hypocenter depth (11 ± 5 km), and a moment magnitude M_w = 4.7, lower than M_w = 5.2 reported by the CMT catalogue. The waveform fits obtained by the CMT inversion are not available (Dziewonski et al. 1987, CMT website) and then it is not possible to compare the quality of solution. We suggest that this difference could be mainly related to the characteristics of the algorithms, the local structure complexities and the different station distributions. In the last years several studies have been performed to compare CMT source parameters with data coming from other moment tensor catalogs (Gasperini et al., 2012; Hjörleifsdóttir and Ekström, 2010; Konstantinou and Rontogianni, 2011). These authors highlighted, in particular, that the CMT algorithm tends to overestimate seismic moment for earthquakes with M_w < 5.0–5.5 occurred before 2003, that is when only the body waves were used for the CMT inversion. Moreover, Hjörleifsdóttir and Ekström (2010) have shown that such overestimate is influenced by local structural setting being more relevant for earthquakes located in a crust thicker than average. This is just the case of the 1978 earthquake located in a region where crustal doubling due to presence of the Ionian subducting slab is testified by seismic tomography results (Di Stefano et al., 2011; Orecchio et al., 2011). These observations may explain the greater magnitude estimate furnished by the CMT analysis with respect to our estimate of M_w 4.7. On this regards, we remark that the *Ferruzzano* earthquake represents one of the smallest earthquakes analyzed through moment tensor inversion of digitized seismograms (Batlló et al., 2010).

7. Conclusions

We studied the 1978 *Ferruzzano* earthquake, that is the most recent moderate-to-major earthquake occurred in the southern Calabria area, by using old analog data and modern inversion techniques. Non-linear earthquake location and waveform inversion of digitized data have allowed us to define new hypocenter location and focal mechanism solution and also to re-assess moment magnitude estimate of the 1978 earthquake. In particular we located the *Ferruzzano* earthquake in the central-eastern portion of the Aspromonte Massif and at shallower depth with respect to previous instrumental location. Normal faulting on ca. N-S oriented fault plane obtained by the time-domain moment tensor inversion well agrees both with the extensional domain defined by seismogenic stress and geodetic strain and with the structural settings proposed by Ghisetti and Vezzani (1981). Waveform inversion have also furnished a moment magnitude of 4.7 quite lower than the previously available estimate of 5.2 coming from the CMT catalog. According to recent studies (Gasperini et al., 2012; Hjörleifsdóttir and Ekström, 2010; Konstantinou and Rontogianni, 2011) we ascribed this overestimate to technical limits of the old CMT approach combined with local structural complexity.

In addition to the intrinsic interest in this earthquake, the 1978 event can be considered a test-case to prove that digitized seismograms may be successfully used to study also relatively small earthquakes (i.e., M_w < 5) of the past. We have shown as the use of modern algorithms in combination with data collected from relatively old instruments may allow to re-evaluate moderate-to-strong earthquakes occurred before

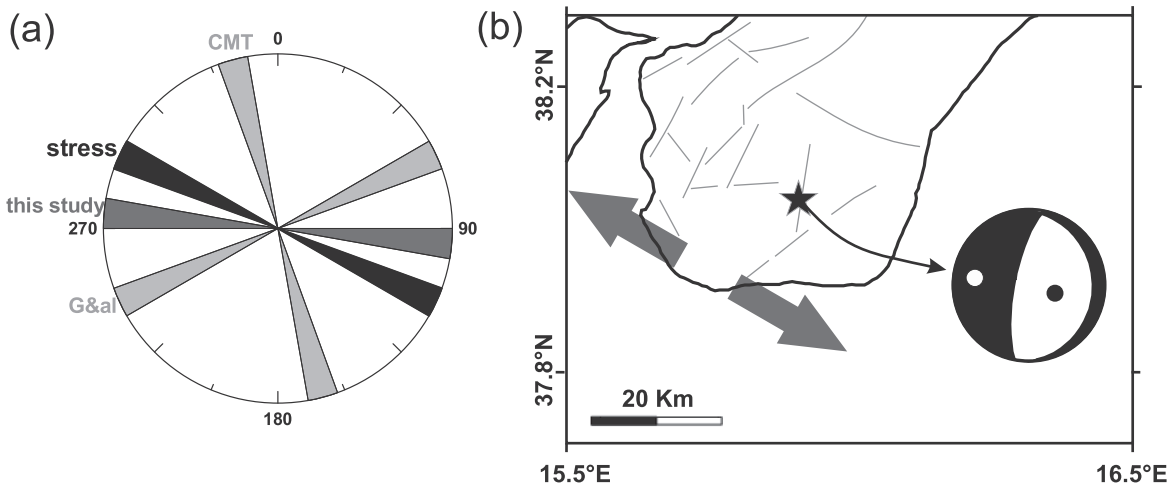

Fig. 7. (a) Rose diagram reporting: in black the σ_3 orientation of the local seismogenic stress field (from Totaro et al., 2016), in dark-gray the T-axis orientations relative to our moment tensor solution (this study), and in light-gray the T-axis orientations relative to the CMT and G&al solutions. It clearly appears that the result obtained in this study is more coherent with the local seismogenic stress field with respect to the previous available solutions. (b) Hypocenter location and focal mechanism solution (with P and T axes) obtained in this study have been reported on the map view of principal structures proposed by Ghisetti and Vezzani (1981). The gray divergent arrows indicate the direction of extension according to seismogenic stress field estimation of Totaro et al. (2016).

the diffusion of modern digital broadband instruments. The good results obtained encourage the use of this approach also to more ancient earthquakes aiming to improve seismotectonics and seismic hazard evaluations in regions of minor recent seismicity.

Acknowledgments

The authors thank Editor and anonymous reviewers for useful comments and suggestions which allowed us to improve the article. We benefit of the historical material recovered and collected by EUROSEISMOS (Ferrari and Pino, 2003) and SISMOS (Michelini et al., 2005) databases. We are also grateful to M. Muga providing us data of the Observatorio Geofísico de Toledo (TOL) and Malaga (MAL).

Appendix A. Supplementary material

Supplementary data to this article can be found online at https://doi.org/10.1016/j.pepi.2019.02.003.

References

Baratta, M., 1907. Il nuovo massimo sismico calabrese (23 ottobre 1907). Boll. Soc. Geog. It. XIII, 1259–1264.
Bassin, C., Laske, G., Masters, G., 2000. The current limits of resolution for surface wave tomography in North America. Eos Trans. AGU, F897 81.
Batlló, J., Bormann, P., 2000. A catalog of old Spanish seismographs. Seismol. Res. Lett. 71, 570–582.
Batlló, J., 2004. Catálogo – Inventario de Sismógrafos Antiguos Españoles. Instituto Geográfico Nacional, Madrid, pp. 414.
Batlló, J., Stich, D., Palombo, B., Macia, R., Morales, J., 2008. The 1951 Mw 5.2 and Mw 5.3 Jaén, Southern Spain, earthquake doublet revisited. B. Seismol. Soc. Am. 98 (3), 1535–1545.
Batlló, J., Stich, D., Macià, R., Morales, J., 2010. Moment tensor inversion for the 5 July 1930 Montilla earthquake (southern Spain). Seismol. Res. Lett. 81 (5), 724–731.
Billi, A., Funiciello, R., Minelli, L., Faccenna, C., Neri, G., Orecchio, B., Presti, D., 2008. On the cause of the 1908 Messina tsunami, southern Italy. Geophys. Res. Lett. 35 (6).
Billi, A., Minelli, L., Orecchio, B., Presti, D., 2010. Constraints to the cause of three historical tsunamis (1908, 1783, and 1693) in the Messina Straits region, Sicily, southern Italy. Seismol. Res. Lett. 81, 907–915.
Billi, A., Faccenna, C., Bellier, O., Minelli, L., Neri, G., Piromallo, C., Presti, D., Scrocca, D., Serpelloni, E., 2011. Recent tectonic reorganization of the Nubia-Eurasia convergent boundary heading for the closure of the western Mediterranean. Bull. Soc. Géol. Fr. 182, 279–303.
Bottari, A., Lo Giudice, E., Nicoletti, P.G., SorrisoValvo, M., 1981. The Ferruzzano earthquake of 1978: macroseismic effects and slope stability conditions in southern Calabria (Italy). Rev. Geol. Dyn. Geogr. 23 (1), 7384.
Bottari, A., Pietrafesa, M., Stillitani, E., 1990. Sull'attenuazione dell'intensità macrosismica nella regione dell'Arco Calabro-Peloritano. Atti del Convegno del GNDT 1, 1–13.
Cadek, O., 1987. Studying earthquake ground motion in Prague from Wiechert seismograph records. Gerl. Beitr. Geoph. 96, 438–447.
Catalano, S., De Guidi, G., Monaco, C., Tortorici, G., Tortorici, L., 2003. Long-term behaviour of the late Quaternary normal faults in the Straits of Messina area (Calabrian Arc): structural and morphological constraints. Quater. Int. 101–102, 81–91.
Chiarabba, C., Palano, M., 2017. Progressive migration of slab break-off along the southern Tyrrhenian plate boundary: Constraints for the present day kinematics. J. Geodyn. 105, 51–61.
Ciaranfi, N., Ghisetti, F., Guida, M., Iaccarino, G., Lambiase, S., Pieri, P., Rapisardi, L., Ricchetti, G., Torre, M., Tortorici, L., Vezzani, L., 1983. Carta neotettonica dell'Italia meridionale. Prog. Fin. Geod. Pub. 515, 1–62.
Crouse, C.B., Matuschka, T., 1983. Digitialization noise and accelerograph pen offset associated with Japanese accelerograms. Bull. Seism. Soc. Am. 73, 1187–1196.
D'Amico, S., Orecchio, B., Presti, D., Zhu, L., Herrmann, R.B., Neri, G., 2010. Broadband waveform inversion of moderate earthquakes in the Messina Straits, southern Italy. Phys. Earth Planet. In. 179, 97–106.
D'Amico, S., Orecchio, B., Presti, D., Gervasi, A., Zhu, L., Guerra, I., Neri, G., Herrmann, R.B., 2011. Testing the stability of moment tensor solutions for small earthquakes in the Calabro-Peloritan Arc region (southern Italy). B. Geofis. Teor. Appl. 52 (2), 283–298.
Deschamps, A., Iannaccone, G., Scarpa, R., 1984. The umbrian earthquake (Italy) of 19 september 1979. Ann. Geophys. 2 (1), 29–36.
DISS Working Group (2015). Database of Individual Seismogenic Sources (DISS), Version 3.2.0: A compilation of potential sources for earthquakes larger than M 5.5 in Italy and surrounding areas, http://diss.rm.ingv.it/diss/, Istituto Nazionale di Geofisica e Vulcanologia; doi:10.6092/INGV.IT-DISS3.2.0.
Di Stefano, R., Bianchi, I., Ciaccio, M.G., Carrara, G., Kissling, E., 2011. Three-dimensional Moho topography in Italy: New constraints from receiver functions and controlled source seismology. Geochem. Geophy. Geosys. 12 (9).
Dziewonski, A.M., Ekström, G., Franzen, J.E., Woodhouse, J.H., 1987. Global seismicity of 1978: centroid-moment tensor solutions for 512 earthquakes. Phys. Earth Planet. In. 46 (4), 316–342.
Faccenna, C., Davy, P., Brun, J.P., Funiciello, R., Giardini, D., Mattei, M., Nalpas, T., 1996. The dynamics of back-arc extension: an experimental approach to the opening of the Tyrrhenian Sea. Geophys. J. Int. 126, 781–795.
Faccenna, C., Piromallo, C., Crespo-Blanc, A., Jolivet, L., 2004. Lateral slab deformation and the origin of the western Mediterranean arcs. Tectonics 23, TC1012. https://doi.org/10.1029/2002TC001488.
Faccenna, C., Molin, P., Orecchio, B., Olivetti, V., Bellier, O., Funiciello, F., Minelli, L., Piromallo, C., Billi, A., 2011. Topography of the Calabria subduction zone (southern Italy): clues for the origin of Mt Etna. Tectonics 30, TC1003. https://doi.org/10.1029/2010TC002694.
Ferrari, G., Pino, N.A., 2003. EuroSeismos 2002–2003 a project for saving and studying historical seismograms in the Euro-Mediterranean area. Geophys. Res. Abs. 5 EAE03-A-05274.
Grabrovec, D., Allegretti, I., 1994. On the digitizing of historical seismograms. Geofizika 11, 27–31.
Galli, P., Galadini, F., Pantosti, D., 2008. Twenty years of paleoseismology in Italy. Earth-Sci. Rev. 88, 89–117.
Galli, P., Molin, D., 2009. Il terremoto del 1905 in Calabria: Revisione della distribuzione degli effetti e delle ipotesi sismogenetiche. Il Quaternario Italian J. Quaternary Sci. 22 (2), 207–234 (in Italian).
Gasparini, C., Iannaccone, G., Scarpa, R., 1985. Fault-plane solutions and seismicity of the Italian peninsula. Tectonophysics 117 (1–2), 59–78.
Gasperini, P., Lolli, B., Vannucci, G., Boschi, E., 2012. A comparison of moment

magnitude estimates for the European—Mediterranean and Italian regions. Geophys. J. Int. 190 (3), 1733–1745.
Ghisetti, F., Vezzani, L., 1981. Contribution of structural analysis to understanding the geodynamic evolution of the Calabrian Arc (Southern Italy). J. Struct. Geol. 3, 371–381.
Ghisetti, F., 1984. Recent deformations and the seismogenic source in the Messina Strait (southern Italy). Tectonophysics 109 (3–4), 191–208.
Herrmann, R.B., 1987. Computer Programs in Seismology. Saint Louis University, St. Louis.
Hjörleifsdóttir, V., Ekström, G., 2010. Effects of three-dimensional Earth structure on CMT earthquake parameters. Phys. Earth Planet. In. 179 (3–4), 178–190.
Jacques, E., Monaco, C., Tapponnier, P., Tortorici, L., Winter, T., 2001. Faulting and earthquake triggering during the 1783 Calabria seismic sequence. Geophys. J. Int. 147 (3), 499–516.
Kanamori, H., 1988. Importance of historical seismograms for geophysical research. In: Historical Seismograms and Earthquakes of the World, pp. 16–33.
Kennett, B.L.N., Engdahl, E.R., Buland, R., 1995. Constraints on seismic velocities in the Earth from traveltimes. Geophys. J. Int. 122 (1), 108–124. https://doi.org/10.1111/j.1365-246X.1995.tb03540.x.
Konstantinou, K.I., Rontogianni, S., 2011. A comparison of teleseismic and regional seismic moment estimates in the European-Mediterranean region. Seismol. Res. Lett. 82 (2), 188–200.
Lay, T., Wallace, T.C., 1995. Modern Global Seismology. Academic Press, San Diego.
Malinverno, A., Ryan, W., 1986. Extension in the Tyrrhenian Sea and shortening in the Apennines as result of arc migration driven by sinking of the lithosphere. Tectonics 5, 227–245. https://doi.org/10.1029/TC005i002p00227.
Michelini, A., De Simoni, B., Amato, A., Boschi, E., 2005. Collecting, digitizing, and distributing historical seismological data. Eos, Transactions, Am. Geophys. Un. 86 (28), 261. https://doi.org/10.1029/2005EO280002.
Monaco, C., Tortorici, L., 2000. Active faulting in the Calabrian Arc and eastern Sicily. J. Geodyn. 29, 407–424.
Murphy, W., 1993. Mechanisms of slope failure during strong ground motion in Southern Italy-some historical evidence. WIT Transactions on The Built Environment 3.
Neri, G., Barberi, G., Orecchio, B., Mostaccio, A., 2003. Seismic strain and seismogenic stress regimes in the crust of the southern Tyrrhenian region. Earth planet. Sci. Lett. 213 (1–2), 97–112.
Neri, G., Barberi, G., Oliva, G., Orecchio, B., 2004. Tectonic stress and seismogenic faulting in the area of the 1908 Messina earthquake, south Italy. Geophys. Res. Lett. 31, 10 0.1029/2004GL019742.
Neri, G., Barberi, G., Oliva, G., Orecchio, B., 2005. Spatial variations of seismogenic stress orientations in Sicily, south Italy. Phys. Earth planet. Inter. 148, 175–191.
Neri, G., Oliva, B., Orecchio, B., Presti, D., 2006. A possible seismic gap within a highly seismogenic belt crossing Calabria and eastern Sicily, Italy. B. Seismol. Soc. Am. 96, 321–331.
Neri, G., Orecchio, B., Totaro, C., Falcone, G., Presti, D., 2009. Seismic tomography says that lithospheric subduction beneath south Italy is close to die. Seismol. Res. Lett. 80, 63–70. https://doi.org/10.1785/gssrl.80.1.63.
Neri, G., Marotta, A.M., Orecchio, B., Presti, D., Totaro, C., Barzaghi, R., Borghi, A., 2012. How lithospheric subduction changes along the Calabrian Arc in southern Italy: geophysical evidences. Int. J. Earth Sci. 101, 1949–1969.
Nocquet, J., 2012. Present-day kinematics of the Mediterranean: A comprehensive overview of GPS results. Tectonophysics 579, 220–242.
Okal, E.A., Reymond, D., 2003. The mechanism of great Banda Sea earthquake of 1 February 1938: Applying the method of preliminary determination of focal mechanism to a historical event. Earth Planet Sci. Lett. 216, 1–15.
Orecchio, B., Presti, D., Totaro, C., Guerra, I., Neri, G., 2011. Imaging the velocity structure of the Calabrian Arc region (South Italy) through the integration of different seismological data. B. Geofis. Teor. Appl. 52, 625–638.
Orecchio, B., Presti, D., Totaro, C., Neri, G., 2014. What earthquakes say concerning residual subduction and STEP dynamics in the Calabrian Arc region, south Italy. Geophys. J. Int. 199, 1929–1942. https://doi.org/10.1093/gji/ggu373.
Palano, M., 2015. On the present-day crustal stress, strain-rate fields and mantle anisotropy pattern of Italy. Geophys. J. Int. 200, 969–985. https://doi.org/10.1093/gji/ggu451.
Pepe, F., Sulli, A., Bertotti, G., Cella, F., 2010. Architecture and Neogene to Recent evolution of the western Calabrian continental margin: An upper plate perspective to the Ionian subduction system, central Mediterranean. Tectonics 29, TC3007. https://doi.org/10.1029/2009TC002599.
Pino, N.A., Palombo, B., Ventura, G., Perniola, B., Ferrari, G., 2008. Waveform modeling of historical seismograms of the 1930 Irpinia earthquake provides insight on "blind" faulting in southern Apennines (Italy). J. Geophys. Res.-Sol. Ea. 113 (B5).
Pino, N.A., Piatanesi, A., Valensise, G., Boschi, E., 2009. The 28 December 1908 Messina Straits earthquake (Mw 7.1): A great earthquake throughout a century of seismology. Seismol. Res. Lett. 80 (2), 243–259.
Pintore, S., Quintiliani, M., Franceschi, D., 2005. Teseo: A vectorizer of historical seismograms. Comp. Geosci. 31, 1277–1285.
Polonia, A., Torelli, L., Artoni, A., Carlini, M., Faccenna, C., Ferranti, L., Gasperini, L., Govers, R., Klaeschen, D., Monaco, C., Neri, G., Nijholt, N., Orecchio, B., Wortel, R., 2016. The Ionian and Alfeo-Etna fault zones: New segments of an evolving plate boundary in the central Mediterranean Sea? Tectonophysics 675, 69–90.
Pondrelli, S., Salimbeni, S., Ekström, G., Morelli, A., Gasperini, P., Vannucci, G., 2006. The Italian CMT dataset from 1977 to the present. Phys. Earth Planet In. 159 (3–4), 286–303.
Presti, D., Troise, C., De Natale, G., 2004. Probabilistic location of seismic sequences in heterogeneous media. B. Seismol. Soc. Am. 94 (6), 2239–2253.
Presti, D., Orecchio, B., Falcone, G., Neri, G., 2008. Linear versus non-linear earthquake location and seismogenic fault detection in the southern Tyrrhenian Sea, Italy. Geophys. J. Int. 172 (2), 607–618.
Presti, D., Billi, A., Orecchio, B., Totaro, C., Faccenna, C., Neri, G., 2013. Earthquake focal mechanisms, seismogenic stress, and seismotectonics of the Calabrian Arc. Italy. Tectonophysics 602, 153–175. https://doi.org/10.1016/j.tecto.2013.01.030.
Presti, D., Neri, G., Orecchio, B., Scolaro, S., Totaro, C., 2017. The 1905 Calabria, Southern Italy, Earthquake: hypocenter location, causative process, and stress changes induced in the area of the 1908 Messina Straits Earthquake. B. Seismol. Soc. Am. 107 (6), 2613–2623.
Riuscetti, M., Schick, R., 1975. Earthquakes and tectonics in southern Italy. Boll. Geof. Teor. Appl. 17 (65), 59–78.
Rosenbaum, G., Lister, G.S., 2004. Neogene and Quaternary rollback evolution of the Tyrrhenian sea, the Apennines, and the Sicilian Maghrebides. Tectonics 23https://doi.org/10.1029/2003TC001518. TC1013.
Rovida, A., Locati, M., Camassi, R., Lolli, B., Gasperini, P., 2016. CPTI15, the 2015 version of the Parametric Catalogue of Italian Earthquakes. Istituto Nazionale di Geofisica e Vulcanologia. https://doi.org/10.6092/INGV.IT-CPTI15.
Sabatini, V., 1908. Appunti sul terremoto calabrese del 23 ottobre 1907, Bollettino del R. Comitato Geologico d'Italia, 1, pp. 3–11.
Scherbaum, F., 1996. Of Poles and Zeros: Fundamentals of Digital Seismology. Kluwer, Dordrecht, The Netherlands.
Schlupp, A., 1996. Néotectonique de la Mongolie Occidentale analysée à partir de données de terrain, sismologiques et satellitaires. PhD thesis. ULP, Strasbourg.
Scognamiglio, L., Tinti, E., Michelini, A., 2009. Real-time determination of seismic moment tensor for the Italian Region. B. Seismol. Soc. Am. 99 (4), 2223–2242. https://doi.org/10.1785/0120080104.
Serpelloni, E., Bürgmann, R., Anzidei, M., Baldi, P., Ventura, B.M., Boschi, E., 2010. Strain accumulation across the Messina Straits and kinematics of Sicily and Calabria from GPS data and dislocation modeling. Earth. Planet. Sc. Lett. 298 (3–4), 347–360.
Snoke, J.A., Lahr, J.C., 2001. Locating earthquakes: At what distance can the earth no longer be treated as flat? Seismol. Res. Lett. 72 (5), 538–541. https://doi.org/10.1785/gssrl.72.5.538.
Stich, D., Batlló, J., Morales, J., Macià, R., Dineva, S., 2003. Source parameters of the 1910 Mw= 6.1 Adra earthquake (southern Spain). Geophys. J. Int. 155, 539–546.
Stich, D., Batlló, J., Macià, R., Teves-Costa, P., Morales, J., 2005. Moment tensor inversion with single-component historical seismograms: The 1909 Benavente (Portugal) and Lambesc (France) earthquakes. Geophys. J. Int. 162 (3), 850–858.
Stich, D., Martín, R., Batlló, J., Macià, R., Mancilla, F., Morales, J., 2018. Normal faulting in the 1923 Berdún earthquake and postorogenic extension in the Pyrenees. Geophys. Res. Lett. 45. https://doi.org/10.1002/2018GL077502.
Tiberti, M.M., Vannoli, P., Fracassi, U., Burrato, P., Kastelic, V., Valensise, G., 2017. Understanding seismogenic processes in the Southern Calabrian Arc: a geodynamic perspective. Ital. J. Geosci 136 (3), 365–388. https://doi.org/10.3301/IJG.2016.12.
Tortorici, L., Monaco, C., Tansi, C., Cocina, O., 1995. Recent and active tectonics in the Calabrian Arc (southern Italy). Tectonophysics 243, 7–55.
Totaro, C., Orecchio, B., Presti, D., Scolaro, S., Neri, G., 2016. Seismogenic stress field estimation in the Calabrian Arc region (south Italy) from a Bayesian approach. Geophys. Res. Lett. 43 (17), 8960–8969.
Valensise, G., Pantosti, D., 2001. The investigation of potential earthquake sources in peninsular Italy: a review. J. Seismol. 5 (3), 287–306.
Van Dijk, J.P., 1992. Late Neogene fore-arc basin evolution in the Calabrian Arc (Central Mediterranean). Tectonic sequence stratigraphy and dynamic geohistory. With special reference to the geology of Central Calabria. Geol. Ultraj. 92 (1992), 288.
Vannoli, P., Vannucci, G., Bernardi, F., Palombo, B., Ferrari, G., 2015. The source of the 30 October 1930 M w 5.8 Senigallia (Central Italy) earthquake: a convergent solution from instrumental, macroseismic, and geological data. B. Seismol. Soc. Am. 105 (3), 1548–1561.
Vannoli, P., Bernardi, F., Palombo, B., Vannucci, G., Console, R., Ferrari, G., 2016. New constraints shed light on strike-slip faulting beneath the southern Apennines (Italy): The 21 August 1962 Irpinia multiple earthquake. Tectonophysics 691, 375–384.